

## ARTICLES

## Deuteron photodisintegration near threshold

M. L. Rustgi and L. N. Pandey

*Physics Department, State University of New York at Buffalo, Buffalo, New York 14260*

(Received 10 April 1989)

The deuteron photodisintegration observables, namely the angular distribution, the total cross section, the ratio ( $\tau$ ) of the photomagnetic and photoelectric components of the total cross section, the ratio of the differential cross section at forward and backward angles to that at  $90^\circ$ , the asymmetry function, and the nucleon polarization near threshold are calculated for several nucleon-nucleon potentials, and their variation with the gamma-ray energy is studied. In the calculations the meson exchange currents and relativistic effects are incorporated. Comparison with the available data is made. It is found that meson exchange currents and relativistic effects manifest themselves more prominently in  $\tau$  and in nucleon polarization than in other observables.

A study of photodisintegration of the deuteron provides an important source of information about the radiative and nucleon-nucleon interaction in the deuteron. Within the framework of the impulse approximation, deuteron photodisintegration below pion threshold has been investigated by many authors.<sup>1-3</sup> However, several years ago, new interest in deuteron photodisintegration was stimulated after the successful resolution of the puzzling discrepancy in  $n$ - $p$  capture at thermal energy by Riska and Brown,<sup>4</sup> who incorporated the contributions from the meson exchange currents and isobar configurations in the magnetic dipole operators. A few years later, it was pointed out by Cambi, Mosconi, and Ricci<sup>5</sup> that relativistic corrections to the impulse approximation must be included to obtain agreement between theory<sup>6-8</sup> and the experimental results of the Mainz group for the forward angle cross section.<sup>9</sup> The results of the Mainz group were later confirmed by measurements done by Dupont *et al.*,<sup>10</sup> Ninane *et al.*,<sup>11</sup> and Meyer *et al.*<sup>12</sup> New measurements on the cross section and polarization asymmetry have been reported by De Pascale *et al.*<sup>13</sup> in the 20–60 MeV  $\gamma$ -ray energy range. Most of this activity in deuteron photodisintegration had been confined to energies well above the photodisintegration threshold.

In the last few years many laboratories have carried out measurements on the angular distribution and total cross section at lower energies. Smit and Brooks<sup>14</sup> have measured the angular distribution of neutrons from deuteron photodisintegration by 2.75 MeV gamma rays because of the increased importance of the meson exchange currents (MEC's) and relativistic effects near threshold. Accurate absolute cross sections were measured by Birenbaum *et al.*<sup>15</sup> at seven photon energies between 6 and 11.4 MeV. Measurements on the ratio of the differential cross section at forward and backward angles to that at  $90^\circ$  have been performed at Argonne National Laboratory.<sup>16</sup> In two theoretical papers,<sup>17</sup> it has been pointed out that the measurement of these ratios project

the effect of the  $E2$  transition, and determination of this amplitude is now feasible provided that we have secure knowledge of the  $E1$  and  $M1$  amplitudes. These studies, along with the measurements on nucleon<sup>18</sup> polarization, suggest that a thorough study of the reaction  ${}^2\text{H}(\gamma, n){}^1\text{H}$  just above threshold is highly desirable and is the subject of this investigation.

A detailed study of the relative importance of the various transitions including  $E1$ ,  $M1$ , and  $E2$  had been carried out by Rustgi, Zernik, Breit, and Andrews<sup>1</sup> (referred to as RZBA in the following; the notation of this paper is followed here). They pointed out that for polarized photons the angular distribution of the outgoing nucleons may be written as

$$\begin{aligned} \sigma(\theta) = & a + b \sin^2\theta \pm c \cos\theta \pm d \cos\theta \sin^2\theta + e \sin^2\theta \cos^2\theta \\ & + \cos 2\phi (f \sin^2\theta \pm d \cos\theta \sin^2\theta + e \sin^2\theta \cos^2\theta), \end{aligned} \quad (1)$$

which gives for the total cross section

$$\sigma_T = 4\pi a + \frac{8\pi}{3} b + \frac{8\pi e}{15}. \quad (2)$$

The plus sign (minus sign) refers to protons (neutrons). Since only  $E1$  and  $M1$  transitions contribute to the cross section at low  $\gamma$ -ray energies near the threshold, following RZBA, we can write for polarized gamma rays

$$\begin{aligned} \sigma(\theta) = & a_E + b_E \sin^2\theta (1 + \cos 2\phi) + a_M \\ & + b_M \sin^2\theta (1 - \cos 2\phi), \end{aligned} \quad (3)$$

and

$$\sigma_T = 4\pi (a_E + \frac{2}{3} b_E + a_M + \frac{2}{3} b_M). \quad (4)$$

It has been known for some time that just above threshold, since  $a_E \ll a_M$  and  $b_M \ll b_E$ , the ratio of the photomagnetic and photoelectric components of the total

cross section is given by

$$\tau = \frac{3a_M}{2b_E} \quad (5)$$

As pointed out by Smit and Brooks,<sup>14</sup> for photon energies greater than 2.4 MeV, the fractional change in  $\tau$  due to MEC contributions will be larger and will provide a more sensitive probe of two-body exchange currents and relativistic effects. Also, as the photon energy is increased, higher multipoles ( $L > 1$ ) may contribute to the angular distribution. The measurements of Holt<sup>19</sup> support this conclusion. Since no explicit calculations on the values of  $\tau$  near threshold have been reported in the literature, in this paper we report the results of calculations carried out with a view to investigate the contributions of higher order multipoles at low incident photon energies to  $\tau$ , to the angular distribution, and to ratio of the laboratory differential cross section at forward and backward laboratory angles to that at  $90^\circ$ . Theoretical results on the asymmetry function and polarization of the outgoing nucleons are also reported.

As it will be interesting to compare the predictions of deuteron photodisintegration observables in the low-energy regime for various two-nucleon potentials, the calculations has been carried out for six potentials, namely, the Yale, modified Hamada-Johnston (HJ), supersoft core potentials A (SSC-A), B (SSC-B), and C (SSC-C), and the Paris potential. The calculations have been carried out to calculate the angular distribution coefficients, polarization, asymmetry function,  $\tau$ , the ratio of the photomagnetic and photoelectric components of the total cross section, and the ratio of the laboratory differential cross sections at  $\theta_{\text{lab}} = 45^\circ, 135^\circ, \text{ and } 155^\circ$ , to that at  $\theta_{\text{lab}} = 90^\circ$  laboratory angles.

Since the main objective of this calculation was to isolate the contributions of the various terms, the calculation was carried out in nine approximations. In approximations I, II, and III, the calculation was performed employing the static  $E1$ ,  $M1$ , and  $E1 + M1 + E2$  multipoles, respectively. In the rest of the calculations, the relativistic<sup>5</sup> and meson exchange contributions<sup>20</sup> were included. In approximations IV, V, and VI, the contributions of the exchange currents using pseudoscalar ( $PS\pi N$ ) coupling were incorporated. The exchange current effects in pseudovector ( $PV\pi N$ ) couplings were incorporated in approximations VII ( $E1$ ), VIII ( $M1$ ), and IX ( $E1 + M1 + E2$ ). Since the pseudoscalar and pseudovector coupling give almost identical results, the results for approximations VII, VIII, and IX are not listed.

The cross section parameters  $a$ ,  $b$ ,  $c$ ,  $d$ , and  $e$ , the total cross section, and  $\tau$  for the Paris potentials are given in Table I. Since the Yale, Hamada-Johnston, SSC-A, SSC-B, and SSC-C give results somewhat similar to that for the Paris potential, we have chosen not to report the results for these potentials. (These results, however, will be made available on request.)

As already stated, the  $PV\pi N$  coupling and  $PS\pi N$  coupling give almost identical results, and a measurement of the photodisintegration observables cannot distinguish between the two types of couplings. For the Paris potential, our values for the coefficient ratios for 2.75 MeV

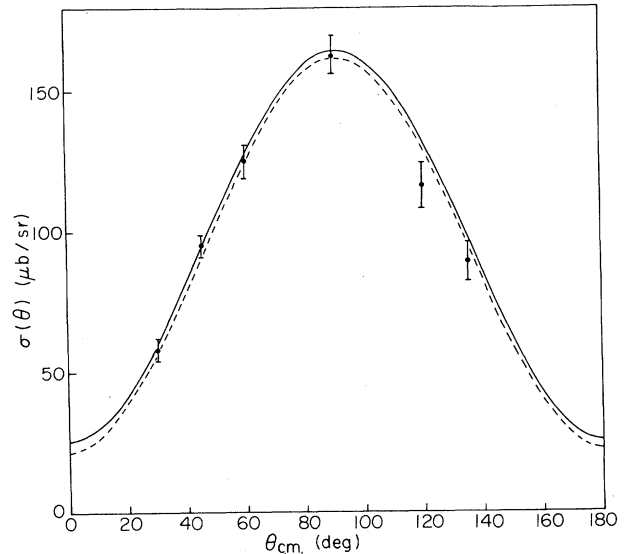


FIG. 1. Comparison of experimental (Ref. 14) and theoretical angular distribution for neutrons using the Paris potential and  $E1 + M1 + E2$  multipoles on including (solid) and excluding (dashed) exchange currents and relativistic effects. The experimental points have been multiplied by 5.44.

gamma rays, not including MEC and relativistic effects, are found to be:  $a/b = 0.164$ ;  $c/b = 0.00001$ ;  $d/b = 0.047$ ;  $e/b = 0.0006$ . On including MEC and relativistic effects, these values change to:  $a/b = 0.184$ ;  $c/b = 0.0000$ ;  $d/b = 0.047$ ;  $e/b = 0.0006$ . These values are in agreement with those of Arenhövel and Miller as reported by Smit and Brooks.

In Fig. 1, the experimental angular distribution of neu-

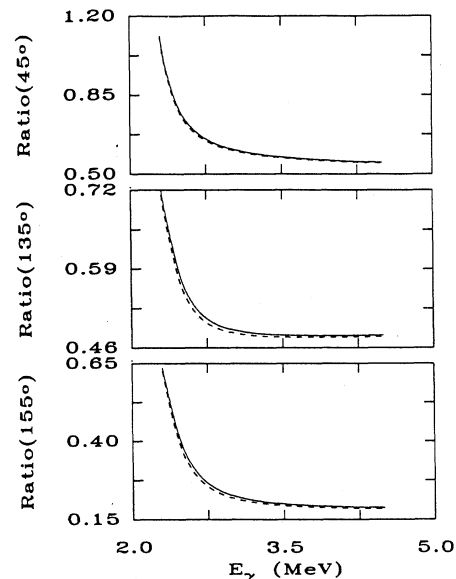


FIG. 2. Ratio of the laboratory cross section at  $45^\circ, 135^\circ$ , and  $155^\circ$  laboratory angles to that at  $90^\circ$  for neutrons for the Paris potential on including (solid) and excluding (dashed) exchange currents and relativistic effects.

TABLE I. Angular distribution parameters in  $\mu\text{b}/\text{sr}$  and total cross section in  $\mu\text{b}$  for protons in approximations I–VI using the Paris potential. For each energy the cross section ratio  $\tau$  in the first row is evaluated using Eq. (5) and in the second row is calculated using  $\sigma(M1)/\sigma(E1)$  without including MEC and relativistic effects. The next two rows present the same ratios when MEC and relativistic effects are included.

$E_\gamma$ (MeV)	Approximation	$a$	$b$	$c$	$d$	$e$	$\sigma_T$	$\tau$
2.300	I	0.0097	12.5970	0.0000	0.0000	0.0000	105.66	5.1982
	II	43.6544	0.0155	0.0000	0.0000	0.0000	548.71	5.1934
	III	43.6641	12.6126	-0.0004	0.2244	0.0010	654.36	
	IV	0.0111	12.6047	0.0000	0.0000	0.0000	105.74	5.7464
	V	48.2881	0.0168	0.0000	0.0000	0.0000	606.95	5.7402
	VI	48.2993	12.6215	-0.0009	0.2245	0.0010	712.69	
2.500	I	0.0600	69.7033	0.0000	0.0000	0.0000	584.70	0.6710
	II	31.1785	0.0473	0.0000	0.0000	0.0000	392.20	0.6708
	III	31.2385	69.7506	-0.0003	2.3879	0.0205	976.93	
	IV	0.0692	69.7584	0.0000	0.0000	0.0000	585.28	0.7477
	V	34.7730	0.0515	0.0000	0.0000	0.0000	437.40	0.7473
	VI	34.8422	69.8100	-0.0019	2.3889	0.0205	1022.71	
2.750	I	0.1368	138.3977	0.0000	0.0000	0.0000	1161.16	0.2442
	II	22.5349	0.0759	0.0000	0.0000	0.0000	283.82	0.2444
	III	22.6717	138.4737	0.0019	6.5581	0.0777	1445.11	
	IV	0.1594	138.5423	0.0000	0.0000	0.0000	1162.65	0.2749
	V	25.3902	0.0835	0.0000	0.0000	0.0000	319.76	0.2750
	VI	25.5496	138.6258	-0.0007	6.5618	0.0777	1482.54	
2.754	I	0.1381	139.3752	0.0000	0.0000	0.0000	1169.36	0.2415
	II	22.4359	0.0763	0.0000	0.0000	0.0000	282.58	0.2417
	III	22.5740	139.4516	0.0020	6.6296	0.0788	1452.07	
	IV	0.1609	139.5215	0.0000	0.0000	0.0000	1170.87	0.2718
	V	25.2827	0.0839	0.0000	0.0000	0.0000	318.42	0.2719
	VI	25.4436	139.6054	-0.0007	6.6333	0.0788	1489.42	
2.900	I	0.1851	172.1124	0.0000	0.0000	0.0000	1444.21	0.1685
	II	19.3342	0.0907	0.0000	0.0000	0.0000	243.72	0.1688
	III	19.5193	172.2032	0.0041	9.2512	0.1243	1688.14	
	IV	0.2167	172.3210	0.0000	0.0000	0.0000	1446.36	0.1908
	V	21.9163	0.1002	0.0000	0.0000	0.0000	276.25	0.1910
	VI	22.1330	172.4212	0.0009	9.2572	0.1243	1722.81	
3.200	I	0.2834	222.4523	0.0000	0.0000	0.0000	1867.17	0.1013
	II	15.0193	0.1173	0.0000	0.0000	0.0000	189.72	0.1016
	III	15.3027	222.5695	0.0099	14.3789	0.2324	257.28	
	IV	0.3342	222.8035	0.0000	0.0000	0.0000	1870.75	0.1160
	V	17.2307	0.1307	0.0000	0.0000	0.0000	217.62	0.1163
	VI	17.5649	222.9342	0.0059	14.3910	0.2324	2088.77	
3.600	I	0.4174	261.6659	0.0000	0.0000	0.0000	2197.37	0.0658
	II	11.4851	0.1483	0.0000	0.0000	0.0000	145.57	0.0662
	III	11.9027	261.8141	0.0199	20.0982	0.3859	2343.59	
	IV	0.4948	262.2248	0.0000	0.0000	0.0000	2203.03	0.0766
	V	13.3856	0.1675	0.0000	0.0000	0.0000	169.61	0.0770
	VI	13.8806	262.3921	0.0153	20.1209	0.3859	2373.29	
4.000	I	0.5557	279.7446	0.0000	0.0000	0.0000	2350.57	0.0494
	II	9.2109	0.1760	0.0000	0.0000	0.0000	117.22	0.0499
	III	9.7669	279.9202	0.0320	24.4269	0.5333	2468.68	
	IV	0.6594	280.5195	0.0000	0.0000	0.0000	2358.36	0.0583
	V	10.9032	0.2011	0.0000	0.0000	0.0000	138.70	0.0588
	VI	11.5629	280.7202	0.0270	24.4627	0.5333	2497.95	

trons measured by Smit and Brooks for 2.75 MeV gamma rays is compared with our theoretical calculations for the Paris potentials. Since these are not absolute measurements, the experimental points of Smit and Brooks had been multiplied by a factor of 5.44 to make the above-mentioned comparison, and good agreement is obtained.

Table I shows the values of the dipole cross section ratio  $\tau$ , the ratio of the photomagnetic and photoelectric components of the total cross section versus the  $\gamma$ -ray energy. It is found that the exchange current contributions enhance  $\tau$  by about 12% at 2.3 MeV, but increase by about 8% at 4.00 MeV. At incident photon energy of 2.75 MeV,  $\tau$  is enhanced by about 10%. Smit and Brooks found the dipole cross section ratio at this energy to be  $\sigma_M/\sigma_E=0.290\pm 0.021$ . The Yale, HJ, Paris, and SSC-B potentials give the value of  $\tau$  as 0.288, 0.281, 0.275, and 0.265, respectively. All are in good agreement with the observed value.

Table I also lists the values of the total cross section. Recently, Moreh, Kennett, and Prestwich<sup>21</sup> measured the absolute cross section of the  ${}^2\text{H}(\gamma, n){}^1\text{H}$  reaction at 2.754 MeV. The measured value is found to be  $1456\pm 45 \mu\text{b}$ . On including exchange effects, our value for the Yale, HJ, SSC-B, and Paris potentials are found to be 1468, 1496, 1523, and 1489  $\mu\text{b}$ , respectively. Except for the SSC-B potential, which gives a slightly higher value, all the remaining potentials are in good agreement with the observed value. These theoretical values differed from each other by about 2%.

Figure 2 shows our theoretical results for the ratio of the laboratory cross section at  $45^\circ$ ,  $135^\circ$ , and  $155^\circ$  laboratory angles to that at  $90^\circ$  for the Paris potential. Smit and Brooks have also calculated the evidence for the

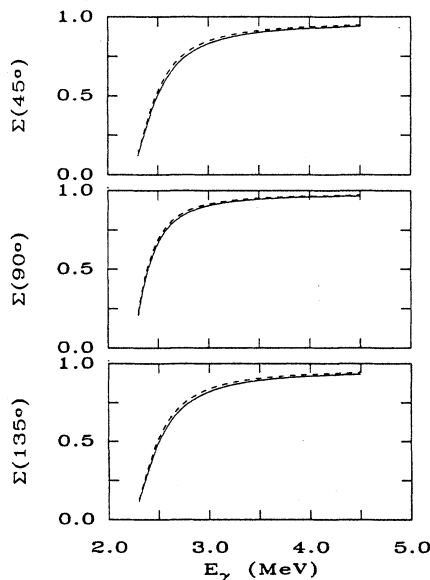


FIG. 3. The asymmetry function versus the gamma-ray energy for neutrons at center-of-mass angles  $45^\circ$ ,  $90^\circ$ , and  $135^\circ$  for the Paris potential on including (solid) and excluding (dashed) exchange currents and relativistic effects.

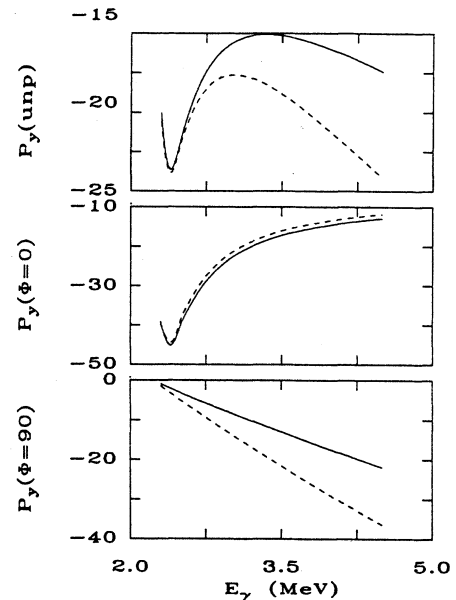


FIG. 4. The  $y$  component of neutron polarization for polarized ( $\phi=0^\circ$  and  $90^\circ$ ) and unpolarized gamma rays versus the gamma-ray energy for the Paris potential. The solid and dotted curves are obtained on including and excluding the exchange currents and relativistic effects, respectively.

asymmetry about  $90^\circ$  from the photoneutron differential cross section  $\sigma(\theta)$  from the ratio  $R(\theta)$  defined by

$$R(\theta) = \sigma(\pi - \theta) / \sigma(\theta). \quad (6)$$

They find from their measurements,  $R(45^\circ) = 0.93 \pm 0.09$  and  $R(60^\circ) = 0.93 \pm 0.06$ . From our calculations, we find

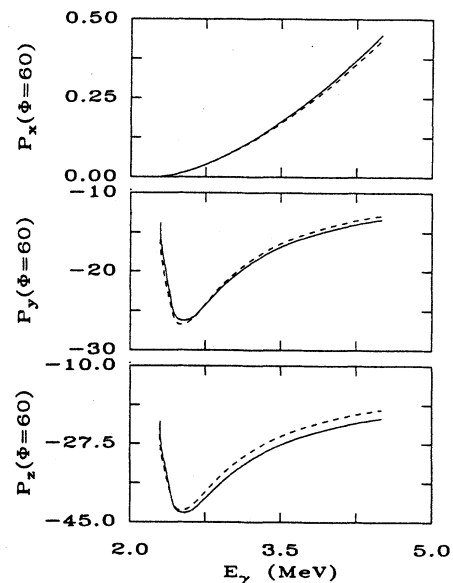


FIG. 5. The neutron polarization components for  $\theta=90^\circ$  employing polarized ( $\phi=60^\circ$ ) gamma rays versus the gamma-ray energy for the Paris potential. The solid and dotted curves are obtained on including and excluding the exchange currents and relativistic effects, respectively.

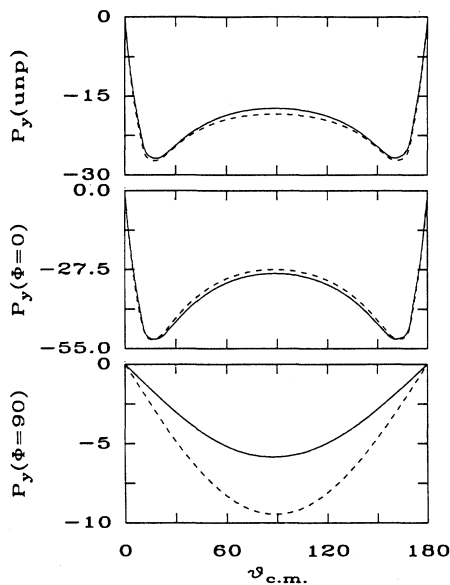


FIG. 6. The neutron polarization vs  $\theta_{c.m.}$  for 2.75 MeV gamma rays for the Paris potential. The solid and dotted curves are obtained on including and excluding the exchange currents and relativistic effects, respectively.

that for all the potentials  $R(45^\circ)=1.05$  and  $R(60^\circ)=1.04$ . The small discrepancy between theory and experiment may not be of much significance.

Figure 3 shows the asymmetry function versus the gamma-ray energy for three center-of-mass angles:  $45^\circ$ ,  $90^\circ$ , and  $135^\circ$ . The  $y$  component of neutron polarization for  $\theta=90^\circ$  for linearly polarized and unpolarized gamma rays versus gamma-ray energy is shown in Fig. 4. The exchange currents manifest themselves very prominently in two of these curves. Similar curves for the three components of neutron polarization for  $\theta=90^\circ$  and  $\phi=60^\circ$  are shown in Fig. 5. The neutron polarization versus the center-of-mass angle for  $E_\gamma=2.75$  MeV for polarized and unpolarized gamma rays is shown in Fig. 6.

It would be desirable to seek experimental confirmation of these results. Our results indicate that various nucleon-nucleon potentials predict the low-energy deuteron photodisintegration observables such as  $\tau$  within 2% of each other. It may be difficult to distinguish between these potentials from these measurements, but the measurements on polarization using polarized gamma rays could provide a valuable tool to determine the contribution of the MEC and relativistic effects.

Some of this work was initiated at the request of Professor R. Moreh, who needed the results for comparison with his new measurements.

- <sup>1</sup>M. L. Rustgi, W. Zernik, G. Breit, and D. J. Andrews, *Phys. Rev.* **120**, 1881 (1960). The notation of this paper is followed here.
- <sup>2</sup>F. Partovi, *Ann. Phys. (N.Y.)* **27**, 79 (1964).
- <sup>3</sup>W. Zickendraht, M. L. Rustgi, and R. G. Brandt, *Nuovo Cimento* **52A**, 247 (1979); R. Botzian, M. L. Rustgi, and A. J. Torruella, *ibid.* **52A**, 309 (1979); M. L. Rustgi, R. D. Nunemaker, and R. D. Sharma, *ibid.* **77A**, 317 (1983). These papers contain a comprehensive list of the earlier references.
- <sup>4</sup>D. O. Riska and G. E. Brown, *Phys. Lett.* **38B**, 193 (1972).
- <sup>5</sup>A. Cambi, B. Mosconi, and R. Ricci, *Phys. Rev. Lett.* **48**, 462 (1982).
- <sup>6</sup>H. Arenhövel and W. Fabian, *Nucl. Phys.* **A282**, 397 (1977).
- <sup>7</sup>E. L. Loman, *Phys. Lett.* **68B**, 419 (1977).
- <sup>8</sup>M. L. Rustgi, T. S. Sandhu, and O. P. Rustgi, *Phys. Lett.* **70B**, 145 (1977).
- <sup>9</sup>R. J. Hughes, A. Ziegler, H. Waffler, and B. Ziegler, *Nucl. Phys.* **A267**, 329 (1976).
- <sup>10</sup>A. Ninane, C. Dupont, P. Leleux, P. Lipnik, and P. Macq, *Can. J. Phys.* **62**, 1104 (1984).
- <sup>11</sup>C. Dupont, P. Leleux, P. Lipnik, P. Macq, and A. Ninane, *Nucl. Phys.* **A445**, 13 (1985).
- <sup>12</sup>H. O. Meyer, J. R. Hall, M. Hugi, H. J. Karwowsky, R. E. Pollock, and P. Schwandt, *Phys. Rev. C* **31**, 309 (1985).
- <sup>13</sup>M. P. De Pascale *et al.*, *Phys. Rev. C* **32**, 1830 (1985).
- <sup>14</sup>F. D. Smit and F. D. Brooks, *Nucl. Phys.* **A465**, 429 (1987).
- <sup>15</sup>Y. Birenbaum, S. Kahane, and R. Moreh, *Phys. Rev. C* **32**, 1825 (1985).
- <sup>16</sup>K. Stephenson, R. J. Holt, R. D. McKeown, and J. R. Specht, *Phys. Rev. C* **35**, 2023 (1987).
- <sup>17</sup>E. Hadjimichael, M. L. Rustgi, and L. N. Pandey, *Phys. Rev. C* **36**, 44 (1987); A. Kassae, L. N. Pandey, M. L. Rustgi, and E. Hadjimichael, *ibid.* **39**, 1147 (1989).
- <sup>18</sup>R. W. Jewell, W. John, and J. E. Sherwood, *Phys. Rev. B* **139**, 71 (1965); R. J. Holt, K. Stevenson, and J. R. Specht, *Phys. Rev. Lett.* **50**, 577 (1983); R. Nath, F. W. K. Firk, and H. L. Shultz, *Nucl. Phys.* **A194**, 49 (1972); M. L. Rustgi, R. Vyas, and M. Chopra, *Phys. Rev. Lett.* **50**, 236 (1983).
- <sup>19</sup>R. J. Holt, *IEEE Trans. Nucl. NS-28*, 1279 (1981).
- <sup>20</sup>M. L. Rustgi, R. Vyas, and O. P. Rustgi, *Phys. Rev. C* **29**, 785 (1984).
- <sup>21</sup>R. Moreh, T. J. Kennett, and W. V. Prestwich, *Phys. Rev. C* **39**, 1247 (1989). The asterisked values of Rustgi *et al.* quoted in Table II of this paper are incorrect. They should be 1523 and 1489 for the SSB and the Paris potentials, respectively. These values differ from those of Arenhövel by about 2%.